2015 International Symposium on Nonlinear Theory and its Applications
NOLTA2015, Kowloon, Hong Kong, China, December 1-4, 2015

Arnold tongues of 2-D Piecewise Constant Driven Oscillator

Hironori Kuriyama† and Tadashi Tsubone‡

†Nagaoka University of Technology
1603-1, Kamitomioka, Nagaoka, Niigata, 940-2188, Japan
Email: s123125@stn.nagaokaut.ac.jp
‡Nagaoka University of Technology
Email: tsubone@vos.nagaokaut.ac.jp

Abstract—In this study, we consider bifurcation phenomena of a two-dimensional piecewise-constant driven oscillator. The system exhibits phase-locking phenomena in a region in the space of parameters. The region is known as Arnold tongues. We propose a novel method in order to analyze piecewise-constant systems with external force. By using the method, we show theoretical result of stability and bifurcation of the piecewise-constant system driven by an external force, especially, we strictly derive boundaries of Arnold tongues.

1. Introduction

In biology and engineering systems, forced synchronization phenomena are often observed [1][2]. It is well known that phase-locked regions called Arnold tongues are often observed in forced synchronization [3]. It is important to analyze Arnold tongues for understanding the forced synchronizations.

In the past, piecewise-linear systems that can obtain explicit solutions in each piecewise-linear regions were often used to consider the synchronization phenomena [4][5]. However, when the solution of the each region connects another one, it is necessary to solve implicit equations. In other words, numerical computations are needed.

For such problems, Tsubone *et al.* have proposed piecewise-constant systems [6]. Piecewise-constant systems governed by piecewise-constant vector fields have straight orbits. Piecewise solutions can be not only determined as linear equations, the connections of solution can be determined as explicit equation. Therefore, it is a good example of analyzing various phenomena. In addition, rigorous analysis method have been proposed [7]. Analysis of piecewise-constant systems with external force are also reported [8]. However, it is not sufficient for consideration of two or more dimensions non-autonomous systems.

In this paper, we consider bifurcation phenomena that occur in a 2-D piecewise-constant driven oscillator. We propose a novel method in order to analyze piecewise-constant systems with external force. By using the method, we show theoretical result of stability and bifurcation of the piecewise-constant system with external force. Furthermore, we strictly derive boundaries of Arnold tongues.

2. 2-D Piecewise-constant Driven Oscillator

Figure 1 shows a circuit schematic diagram of a 2-D piecewise-constant driven system. The circuit consists of two capacitors, one VCCS having a signam characteristic as shown in Fig. 2(a), two VCCSs having a hysteresis characteristic as shown in Fig. 2(b), and an independent current source.

The circuit dynamic is represented as follows.

$$\begin{cases} C_1 \dfrac{\mathrm{d}v_1}{\mathrm{d}t} = I_1 \cdot H(v_1) + I_3 \cdot \mathrm{sgn}(v_2), \\ C_2 \dfrac{\mathrm{d}v_2}{\mathrm{d}t} = I_2 \cdot H(v_1) + I_4 \cdot B(T,t), \end{cases} \quad (1)$$

where $B(T,t)$ is a current source as shown in Fig. 3, sgn(.) and $H(.)$ are voltage control current sources (VCCSs) that have characteristic as shown in Fig. 2(a) and 2(b), respectively.

$$B(T,t) = \begin{cases} 1, & \text{for } nT \le t < \dfrac{(2n+1)}{2}T, \\ -1, & \text{for } \dfrac{(2n+1)}{2}T \le t < (n+1)T. \end{cases} \quad (2)$$

In order to realize oscillation behavior, we consider following conditions.

$$I_2 = -I_3,\ I_1 \cdot I_2 < 0. \quad (3)$$

Here, by using the following normalized variables and parameters

$$\tau = \frac{I_2}{C_1 v_{th}}t,\ x = \frac{1}{t_{th}}v_1,\ y = \frac{C_2}{C_1 v_{th}}v_2, \\ \alpha = -\frac{I_1}{I_2},\ \beta = \frac{I_4}{I_2},\ T' = \frac{I_2}{C_1 v_{th}}T, \quad (4)$$

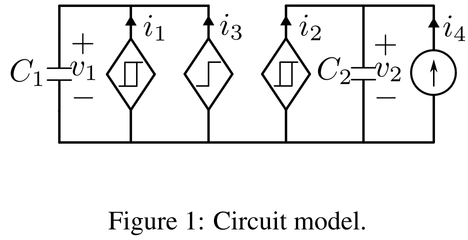

Figure 1: Circuit model.

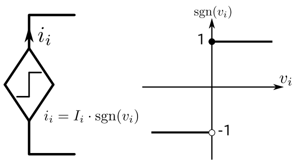

(a) VCCS with Signum-like function.

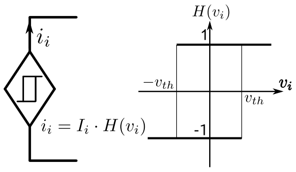

(b) VCCS with hysteresis characteristic.

Figure 2: Symbols and nonlinear characteristics of VCCSs.

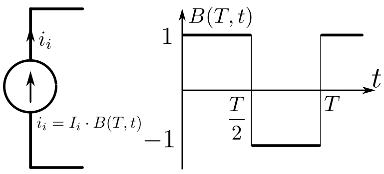

Figure 3: Independence current source.

we can rewrite the circuit dynamics by following normalized equations,

$$\begin{cases} \dot{x} = -\alpha \cdot h(x) - \mathrm{sgn}(y), \\ \dot{y} = h(x) + \beta \cdot B(T', \tau), \end{cases} \tag{5}$$

where "·" denote differentiation by normalized time τ and h is a normalized hysteresis. h is switched from 1 to -1 if x reaches to the threshold -1 and h is switched from -1 to 1 if x reaches to 1. Here, we assume a following parameter conditions.

$$0 < \alpha < 1 \text{ and } 0 < \beta < 1. \tag{6}$$

The condition (6) guarantees oscillatory dynamics. Typical attractors are shown in Fig. 4.

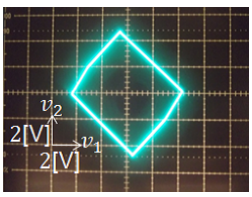

(a) $\beta \cong 0.2, T' \cong 35$ (periodic orbit).

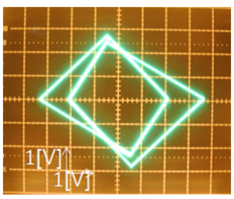

(b) $\beta \cong 0.2, T' \cong 60$ (periodic orbit).

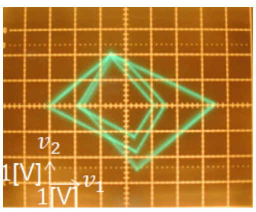

(c) $\beta \cong 0.37, T' \cong 50$(chaos).

Figure 4: Typical attractors ($\alpha \cong 0.2$).

3. Analysis Method

In order to analysis, we derive a novel calculation algorithm for rigorous solutions. In our previous work [7], the basic algorithm depends on 2-D mapping procedure related to state variables. However, the algorithm is not suitable for non-autonomous system, because it can not manage enforced switching depending on external force. So, we propose a novel algorithm based on 3-D mapping with time variable τ.

Step 1.
We set the initial state $\boldsymbol{x}_0$ and get the dependent variable l_0.

$$l_k = \frac{-B(T', \tau) + 1}{2} \cdot 2^2 + \frac{-h(x) + 1}{2} \cdot 2^1 + \frac{-\mathrm{sgn}(y) + 1}{2} \cdot 2^0, \tag{7}$$

where $k = 0$ and x_k, y_k and τ_k denote the elements of $\boldsymbol{x}_k$, that is , $\boldsymbol{x}_k = {}^t(x_k, y_k, \tau_k)$.

Step 2.
We calculate a time τ_k until the l_k switches to l_{k+1}. Assuming a trajectory started from $\boldsymbol{x}_k$ arrives one of thresholds $D_x(l_k), D_y(l_k)$ and $D_\tau(l_k)$, each arrival times τ_x, τ_y and τ_τ are given by

$$\tau_x = \frac{D_x(l_k) - x_k}{a_x(l_k)}, \ \tau_y = \frac{D_y(l_k) - y_k}{a_y(l_k)}, \tag{8}$$

$$\tau_\tau = D_\tau(l_k) - \tau_k \bmod T', \tag{9}$$

where $a_x(l_k)$ and $a_y(l_k)$ denote the elements of $\boldsymbol{a}(l_k)$, that is, $\boldsymbol{a}(l_k) = {}^t(a_x(l_k), a_y(l_k), a_\tau(l_k))$ and $\boldsymbol{a}(l_k)$ is obtained from Table 1. The actual arrival time τ_k that means the switching time of l_k is given by the minimum of τ_x, τ_y and τ_τ omitting zero and negative.

$$\tau_k = \min\{\{\tau_x, \tau_y, \tau_\tau\} \cap \{\xi \in \boldsymbol{R} | \xi > 0\}\}. \tag{10}$$

If all of τ_x, τ_y and τ_τ are not positive, it means that the switching of l_k does not occur. In such case, the trajectory must diverge. However, the situation never happens on the parameter conditions (6).

Step 3.
We calculate $\boldsymbol{x}_{k+1}$ by

$$\boldsymbol{x}_{k+1} = \boldsymbol{x}_k + \boldsymbol{a}(l_k) \cdot \tau_k. \tag{11}$$

We get the integer variable l_{k+1} after switching.

Step 4.
Let $\boldsymbol{x}_{k+1}$ and l_{k+1} be replaced with $\boldsymbol{x}_k$ and l_k, respectively. Subsequently, return to Step 2.

Here, we show an example of local maps in the case where l_k change from 0.

Table 1: Local vector fields and threshold for l

l	$B(T',\tau)$	$h(x)$	sgn(y)	$\boldsymbol{a}(l)$	$D_x(l)$	$D_y(l)$	$D_\tau(l)$
0	1	1	1	${}^t\begin{pmatrix}-\alpha-1 & 1+\beta & 1\end{pmatrix}$	-1	0	$T'/2$
1	1	1	-1	${}^t\begin{pmatrix}-\alpha+1 & 1+\beta & 1\end{pmatrix}$	-1	0	$T'/2$
2	1	-1	1	${}^t\begin{pmatrix}\alpha-1 & -1+\beta & 1\end{pmatrix}$	1	0	$T'/2$
3	1	-1	-1	${}^t\begin{pmatrix}\alpha+1 & -1+\beta & 1\end{pmatrix}$	1	0	$T'/2$
4	-1	1	1	${}^t\begin{pmatrix}-\alpha-1 & 1-\beta & 1\end{pmatrix}$	-1	0	T'
5	-1	1	-1	${}^t\begin{pmatrix}-\alpha+1 & 1-\beta & 1\end{pmatrix}$	-1	0	T'
6	-1	-1	1	${}^t\begin{pmatrix}\alpha-1 & -1-\beta & 1\end{pmatrix}$	1	0	T'
7	-1	-1	-1	${}^t\begin{pmatrix}\alpha+1 & -1-\beta & 1\end{pmatrix}$	1	0	T'

$$\boldsymbol{a}(0) = \begin{pmatrix} a_x(0) \\ a_y(0) \\ 1 \end{pmatrix} = \begin{pmatrix} -\alpha-1 \\ 1+\beta \\ 1 \end{pmatrix}. \tag{12}$$

- Switched $h(x)$

$${}^t\boldsymbol{n} = \begin{pmatrix} 1 & 0 & 0 \end{pmatrix},\ D = D_x(0) = -1, \tag{13}$$

$$\boldsymbol{x}_{i+1} = \begin{pmatrix} 0 & 0 & 0 \\ -\dfrac{1+\beta}{-\alpha-1} & 1 & 0 \\ -\dfrac{1}{-\alpha-1} & 0 & 1 \end{pmatrix} \boldsymbol{x}_i + \begin{pmatrix} -1 \\ -\dfrac{-1+\beta}{-1-\alpha} \\ -\dfrac{1}{-1-\alpha} \end{pmatrix}. \tag{14}$$

- Switched sgn(y)

$${}^t\boldsymbol{n} = \begin{pmatrix} 0 & 1 & 0 \end{pmatrix},\ D = D_y(0) = 0, \tag{15}$$

$$\boldsymbol{x}_{i+1} = \begin{pmatrix} 1 & -\dfrac{-\alpha-1}{1+\beta} & 0 \\ 0 & 0 & 0 \\ 0 & \dfrac{-1}{1+\beta} & 1 \end{pmatrix} \boldsymbol{x}_i. \tag{16}$$

- Switched $B(T',\tau)$

$${}^t\boldsymbol{n} = \begin{pmatrix} 0 & 0 & 1 \end{pmatrix},\ D = D_\tau(0) = \frac{T'}{2}, \tag{17}$$

$$\boldsymbol{x}_{i+1} = \begin{pmatrix} 1 & 0 & -(-\alpha-1) \\ 0 & 1 & -(1+\beta) \\ 0 & 0 & 0 \end{pmatrix} \boldsymbol{x}_i + \begin{pmatrix} (-\alpha-1)\dfrac{T'}{2} \\ (1+\beta)\dfrac{T'}{2} \\ \dfrac{T'}{2} \end{pmatrix}. \tag{18}$$

To analyze periodic orbit, we define Poincare map F_p.

$$S_p = \{\boldsymbol{x} \mid \tau = nT'\}, \tag{19}$$
$$F_p : S_p \to S_p, \tag{20}$$
$$(x_{n+1}, y_{n+1}, (n+1)T') = F_p(x_n, y_n, nT'). \tag{21}$$

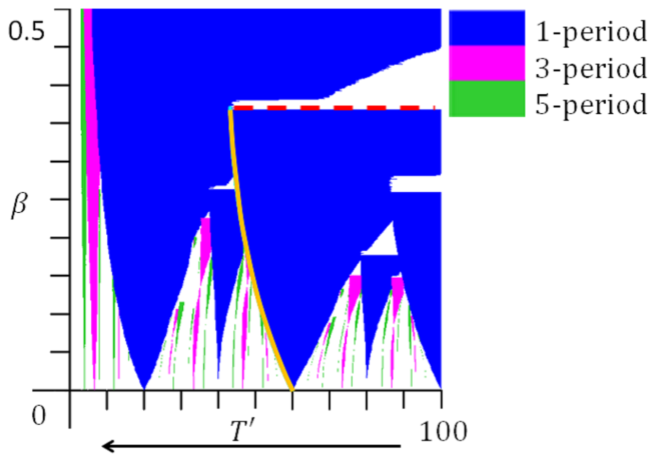

Figure 5: Bifurcation diagram($\alpha = 0.2$).

F_p is defined as composite mapping of local maps. For Poincare map F_p, we define period m.

$$(x_n, y_n, (n+m)T') = F_p^m(x_n, y_n, nT') \tag{22}$$

Bifurcation diagram is shown in Fig.5. Black arrow means flow of parameter change.

3.1. Bifurcation phenomena

We consider bifurcation phenomena when parameter values of β and T' are changed, respectively.

- Change β

  Stability are determined by eigenvalues λ of Jacobian from Poincare map F_p. If moduli of λ are all less than 1, the periodic orbit is stable; otherwise, it is unstable. Eigenvalues of Fig.4(b) ($\beta = 0.2, T' = 60$) are

$$\lambda = \begin{pmatrix} 0.0308 - 0.5434i \\ 0.0308 + 0.5434i \\ 0 \end{pmatrix}. \tag{23}$$

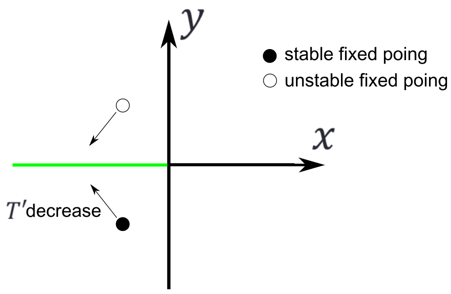

Figure 6: Movement of fixed points.

Eigenvalues of Fig.4(c) ($\beta = 0.37, T' = 50$) are

$$\lambda = \begin{pmatrix} 1.0366 \\ 0.0846 \\ 0 \end{pmatrix}. \tag{24}$$

Therefore, Fig.4(b) is stable and 4(c) is unstable. There is saddle-node bifurcation because one of eigenvalues crosses real value 1.

- Change T'

  The fixed points are determined by

$$(x_n, y_n, (n+1)T') = F_p(x_n, y_n, nT'). \tag{25}$$

  Movement of fixed points, when T' is decreased, is shown in Fig.6. Fixed point hits border $y = 0$ that switches sgn(y). Then, border-collision bifurcation happens. From $y_n = 0$, bifurcation set of border-collision bifurcation is

$$T' = \frac{4(3\alpha^2+1)(\beta^2-1) - 32\alpha\beta}{(\beta^2-1)(\beta(3\alpha^2+1)+\alpha(\alpha^2+3))}. \tag{26}$$

  On $y_n = 0$, Non-smooth saddle-node bifurcation happens because stable fixed point encounters unstable fixed point. Therefore, co-dimensional 2 bifurcation arises on the bifurcation set.

4. Conclusion

In the paper, we considered bifurcation phenomena that occur in a 2-D piecewise-constant oscillator. We proposed a novel method for piecewise-constant system with external force. By using the method, bifurcation phenomena from 2-D piecewise-constant driven oscillator were analyzed. Boundaries of Arnold tongues from the system were derived.

References

[1] K. Tsumoto, T. Yoshinaga, H. Iida, H. Kawakami, K. Aihara, “Bifurcations in a mathematical model for circadian oscillations of clock genes,” Journal of Theoretical Biology 239, pp. 101-122, 2006

[2] Guevara, M.R., Glass, L. and Shrier, A., “Phase locking, period-doubling bifurcations, and irregular dynamics in periodically stimulated cardiac cell,” Science, 214(4527), pp. 1350-1353, 1981.

[3] Y. Kaznelson, “Sigma- finite- invariant measure smooth mapping on the circle,” J. Anal. Math., vol.31, pp.1-8, 1977

[4] Yibo Zhao, Jiuchao Feng, Chi K. Tse, “Stability Analysis of Periodic Orbits of Nonautonomous Piecewise-Linear Systems by Mapping Approach,” IEEE Trans. on Circuits and Systems II Express Briefs, Vol.56, No. 11, pp.845-849, 2009

[5] N. Inaba, N. Baba, M. Ohnishi, “Bifurcation Sets in the Forced Rayleigh Oscillator with a Diode,” IEICE, Trans. Fundamentals (Japanese Edition), Vol.J78-A, No.4, pp.485-492,1995

[6] T. Tsubone, T. Saito, “Manifold Piecewise Constant Systems and Chaos,” IEICE, Trans. Fundamentals, Vol. E82-A, No.8, pp. 1619-1626, 1999

[7] K. Suzuki, T. Tsubone, “In-Phase and Anti-Phase Synchronization Phenomena in Coupled Systems of Piecewise Constant Oscillators,” IEICE, Trans. Fundamentals, Vol. E98-A, No.1, pp340-353, 2015

[8] T. Tsubone, N. Inaba, T. Tsubouchi, T. Yoshinaga, “Synchronization Phenomena from an Extremely Simplified Piecewise-Constant Driven Oscillator,” IEICE Trans. Fundamentals (Japanese Edition), Vol.J93-A, No.5, pp.375-383, 2010